A review of the High-speed Permanent Magnet Rotor Stress Analysis used for Automotive Air-handling Machines

Levi R. Mallin, and Simon M. Barrans

***Abstract*—Machines incorporating high-speed electrical machines (HSEM) are becoming increasingly common place in applications including air handling, energy storage and medical devices. They are of increasing interest within the automotive field for air handling applications. HSEM's use surface-mounted permanent magnet (PM) rotors, manufactured from rare earth metals. However, these PM's have low tensile strength and are susceptible to failure under the centrifugal load produced at high speed rotation. Retaining sleeves which are an interference fit around the magnets, provide compression and hence resistance to tensile stress. The ability to predict the stresses within the rotor assembly is essential for robust design. This review paper examines existing analytical calculations and finite element analysis (FEA) models. The analytical approaches include both plane stress and plane strain models and the limitations of these are discussed. For relatively long rotors, a generalised plane strain approach is suitable, however it is seldom used. In addition, this latter approach has not been extended to assemblies where the magnets are assembled onto a carrier or shaft. Optimisation of rotors has been addressed in a relatively small number of papers. However, further work is required in this area to ensure that the optimised rotors can be manufactured.**

***Index Terms*—High-Speed Electric Machines, Surface-Mounted Permanent Magnet Rotor, Generalised Plane Strain, Plane Stress, Compound Cylinder.**

I. Introduction

Reference [1] discussed how HSEM usage has increased over the last decade due to the performance benefits over mechanical transmission. Efficiency [1]-[3]; reliability, power density, weight and size [4], [5] all improve with HSEM's. As stated by [6], [7], HSEM's rotate via electromagnetic forces, improving reliability over parts in contact, while PM's provide an increase in power density. Sintered PM's such as Samarium Cobalt (SmCo, $SmCo_5$ or Sm_2Co_{17}) or Neodymium ($Nd_2Fe_{14}B$) are used [8]. These high-energy density magnets enable a rotor size reduction and an increase in operating speed [9].

Reference [9] listed compressors, vacuum pumps, turbine generators and medical drills as HSEM applications while [7] included fuel pumps and turbochargers, all of which operate above 10,000 rpm. Reference [10] stated the benefit of HSEM's in dental drills is more user control and [11] discusses how integrating a HSEM and a flywheel can be used as a means of energy storage. Weight and volume savings enable the improvement of energy storage density.

Published on April 19, 2020.
Authors are with University of Huddersfield, UK.

A particularly demanding but potentially large market for HSEM's is within automotive air-handling machines, such as electrically assisted turbochargers. In light-duty vehicles, mechanical turbochargers are used to reduce exhaust emissions. As [12] explained, light-duty vehicles produce 15% of all EU CO_2 emissions and targets are set at a 70% reduction by 2050. Turbochargers extract waste energy

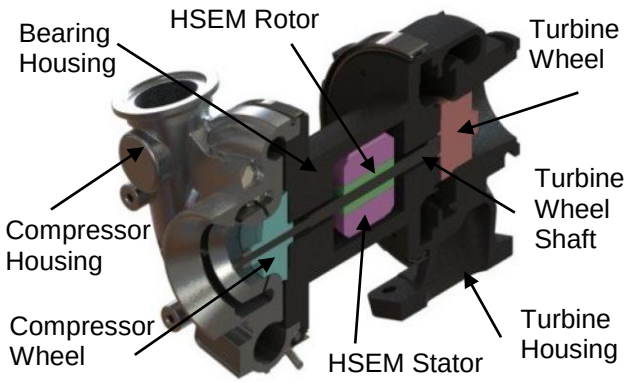

Fig.1. Electric assisted turbocharger, adapted from [13]

from exhaust gases via a turbine connected to a compressor wheel. The compressor wheel draws in air and delivers it to the engine above ambient density for complete fuel combustion, maximising power and enabling engines to be 'down-sized', as discussed by [14]. This air handling control also results in increased engine efficiency and reduced emissions [10]. However, [14] stated slow transient response at low engine speeds caused by insufficient exhaust gas is a drawback to the turbocharger system.

Electric assisted turbochargers (EATs), shown in *Fig.1*, utilise an electric motor to achieve optimum operating speed at low engine speeds, improving slow transient response. As stated by [13], EATs therefore improve engine power density more than mechanical turbochargers. The speed and size requirements of EATs for light-duty vehicles makes application difficult, as discussed by [8]; operating speed requirements are 100-300 krpm whilst dimensions must be minimised to fit within the limited engine space.

II. Rotor Types

Reference [8] defined 'interior' (IPM) and 'surface-mounted' (SPM) as the two configurations of PM rotors, shown in *Fig.2* and *Fig.3*. IPM rotors have PMs buried within the shaft or rotor iron while SPM rotors have PMs glued to the surface, compressed via a retaining sleeve. SPM topologies exist where no distinction between the shaft and rotor iron is made, therefore just a shaft is present as shown

in [15]. [16]-[18] acknowledged that the stress concentrations generated within IPM rotors due to the magnet slots, limit operating speeds. SPM rotors do not contain these stress concentrating features. Therefore [16], [18] recommended SPM rotors for high speed applications despite losses in efficiency due to the retaining sleeve acting as an electromagnetic air gap [8]. Both IPM and SPM rotors are

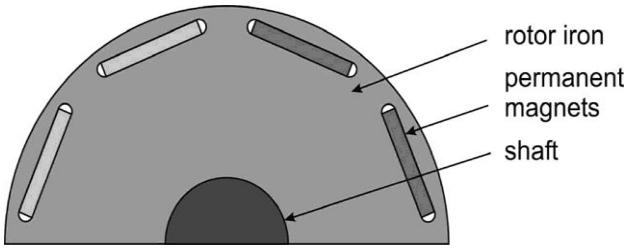

Fig. 2. IPM rotor [16]

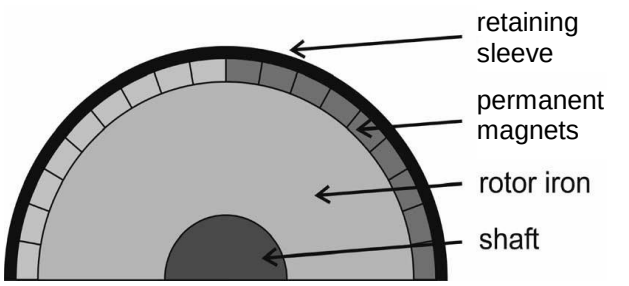

Fig. 3. SPM rotor, adapted from [16]

synchronous which were found by [19] to be the most efficient and power dense type of rotor, further supporting the choice of SPM rotors.

References [8], [18] stated that due to the sintering manufacturing process used in the manufacture of Samarium Cobalt and Neodymium magnets, they have low tensile strength. The retaining sleeve keeps the magnets in compression to counter the tensile stresses generated during operation. This is a critical factor for rotor durability, so the stress analysis must be accurate. This paper will review current stress analysis techniques.

I. Classical Closed-form Analysis Techniques

To apply closed-form analysis techniques to SPM rotor design, approximations are required regarding rotor behaviour. Existing papers differ amongst three main areas of approximation: state of the stress-strain field; impact of thermal effects; and the use of compound cylinder theory.

For the stress-strain field, one of three assumptions will be used: plane stress; plane strain; or generalised plane strain.

Reference [20, p. 254] states a plane body is when two parallel planes are bounded by a closed surface. This applies to cylindrical rotors where the end faces are the parallel planes. [20, p. 255] explains that, in relation to the diameter, a very short cylinder (i.e. a disk) is suitable for plane stress analysis whereas a long cylinder is suitable for plane strain. To apply this, certain assumptions are made:

- No load must be placed on the plane body parallel planes. This would be the axial direction for the rotor.
- Hoop and radial stresses must be uniform throughout the plane body thickness, or over the length in the case of a rotor.

It is important to note that although [20, p. 256] cites rotating cylinders as an example of plane strain, the equations derived from [20, p. 124-125] assume generalized plane strain. This does not require either axial stress or axial strain to be known in order to determine the radial and circumferential stresses. So, whilst the theory presented is applicable to a state of plane strain (i.e. where there is no change in axial dimension), it is not restricted to that case.

The relationship between stress and strain in the rotor is given by the general constitutive relationship expressed in cylindrical coordinates as:

$$\begin{bmatrix}\varepsilon_r\\ \varepsilon_\theta\\ \varepsilon_z\end{bmatrix}=\begin{bmatrix}\frac{1}{E} & -\frac{v}{E} & -\frac{v}{E}\\ -\frac{v}{E} & \frac{1}{E} & -\frac{v}{E}\\ -\frac{v}{E} & -\frac{v}{E} & \frac{1}{E}\end{bmatrix}\begin{bmatrix}\sigma_r\\ \sigma_\theta\\ \sigma_z\end{bmatrix} \quad (1)$$

Where ε_r, ε_θ and ε_z are the strains in the radial, circumferential and axial directions; σ_r, σ_θ and σ_z are the equivalent stress components. E is the Young's modulus of the material and ν is the Poisson's ratio.

However, plane stress assumes the axial stress in the rotor is zero and axial strain is present, i.e.:

$$\sigma_z = 0 \quad (2)$$

$$\varepsilon_z \neq 0 \quad (3)$$

Plane strain assumes axial strain is zero, meaning the rotor is fixed axially by a rigid body. This is unrealistic as no structure has a sufficiently greater stiffness than the rotor to be regarded as rigid. However, plane strain acknowledges the presence of axial stress. Reference [9] represented this as:

$$\sigma_z \neq 0 \quad (4)$$

$$\varepsilon_z = 0 \quad (5)$$

Reference [8] used generalised plane strain which acknowledges axial stress and strain, but assumes axial strain is constant in the rotor.

$$\sigma_z \neq 0 \quad (6)$$

$$\varepsilon_z \neq 0 \quad (7)$$

$$\frac{d\varepsilon_z}{dr} = 0 \quad (8)$$

In previous work, the plane stress assumption was the most common approach, used by [15], [21]-[37], but only justified by [21], [24], [26]. Reference [26] justified plane stress due to a small axial load, while [24] stated it was zero. Reference [21] found minimal difference between plane stress and plane strain results and chose plane stress for simplicity. Although overall axial stress will be zero, [8] observed that due to differential axial deformation during

rotation, axial loads will be present on each cylinder, acting in opposite directions to maintain equilibrium. The presence of axial stress may lead to unreliable predicted values when plane stress is assumed.

References [22], [27]-[31], [33], [35]-[37] used plane stress but did not specify that they had done so. To show how the calculations were conducted, [31] and [37] referenced [29] and [27] respectively. It is unclear if the papers were referenced for using plane stress calculations. Only [3] referenced a paper, [21], which justified the use of plane stress. Reference [3] discussed a segmented magnet rotor design and therefore referenced [16], [38]. However, [16], [38] did not specify the assumptions underpinning their theoretical approach and will be discussed later in this section.

References [9], [39], [40] were the only papers reviewed to use plane strain methodology to calculate interfering cylinder stresses. This method assumes there is no axial strain acting on the cylinders. The rotor topology in [39] was the shaft, magnets and sleeve arranged as three concentric cylinders. However, the analytical equations only related to the interfering magnets and sleeve. As discussed later, analytical calculations of three interfering cylinders was rarely attempted. Reference [9] included stress equations for three cylinders and stated the use of the plane strain assumption. Reference [40] also appears to state a different assumption to the one used in the equations. The plane stress assumption was stated by [40] but the stress equations correspond to the plane strain assumption. Also, [40] did not acknowledge the interference between cylinders so results may differ from a rotor with interference.

Generalised plane strain, as used by [8], acknowledges axial stress and assumes axial strain is constant throughout the body. This creates a more complex theory over plane stress and plane strain, but still generates a closed form solution. According to [8], axial stresses become more concentrated at the rotor ends when friction between the bodies increases. Reference [18] corroborated this by observing that shear stresses induced at the rotor ends caused magnet failure. Reference [41] sourced generalised plane strain equations from [42] to compare Von Mises stress across rotor configurations but excluded stresses due to interference.

References [10], [16], [38], [43]-[52] were not categorised either because the theoretical assumptions were not clear or because they did not use one of the three main methods above. The complex approach using both thin cylinder and thick walled cylinder equations proposed by [16] requires careful study to ensure that all the embedded assumptions remain valid. A thin cylinder approximation assumes the cylinder is thin (relative to its diameter) and has constant axial and circumferential stresses through the wall thickness, while neglecting radial stress. Thick cylinder equations correctly acknowledge stress variation through the wall thickness.

Reference [52] stated the thin cylinder equation for their analytical methodology, but showed no further equations. Also, the rotor dimensions used in [52] do not appear to be suitable to the thin cylinder theory due to the sleeve thickness. [10], [50], [51] all referenced [52] for analytical calculations and are therefore subject to the limitations of thin cylinder theory.

When calculating sleeve circumferential stress due to the shrink fit assembly, [16] assumed the sleeve to be a thin cylinder. The thin cylinder assumption remained when the contact pressure (due to shrink fit) between the magnets and sleeve was calculated. This contact pressure was also assumed to be acting at the back-iron to magnet interface. This approximation is reasonable for situations where the thickness of the magnets is small compared to their radius and many, small, separated magnets are distributed around the back-iron. For thicker sleeves, [16] calculated the contact pressure using a thick cylinder equation, but this equation used the circumferential stress previously calculated with the thin walled cylinder assumption. Reference [16] used thin magnets and a thin sleeve and hence their approximations were reasonable. However, this approach would lead to potentially significant errors for: cylindrical or thick magnets; or thick sleeves.

For circumferential stress due to rotation, [16] used a thick walled cylinder approach with what appears to be the plain strain assumption. Whilst a Poisson's ratio was not specified in the equations, it can be calculated that a value of 0.231 was consistently assumed. Work using this equation for materials with a different Poisson's ratio will therefore be in error. Also, [16] discussed glass fibre and carbon fibre retaining sleeves which would cause errors with this equation as they require different Poisson's ratios.

Reference [16] presented equations calculating centripetal force, each on the magnets and the sleeve, at a given radius. The equations will give reasonable approximations if the magnets are considered thin independent blocks and if the sleeve is considered thin. Calculations using these equations will generate errors if these conditions are not met. Papers [3], [43]-[45], [48], [49], [53], [54] all referenced [16] to calculate stress.

References [43], [48] referenced stress equations directly from [16], but [43] used a titanium sleeve with 0.33 Poisson's ratio while [48] used a material with a Poisson's ratio of 0.3. Reference [44] also used the same analytical model as [16] but used glass-fibre and carbon-fibre as sleeve materials with a Poisson's ratio of 0.22 and 0.199 respectively. These sleeve materials used by [44] are composites but they failed to acknowledge Poisson's ratio being directional in anisotropic materials. Reference [49] used [16]'s thick cylinder contact pressure equation (requiring thin magnets) and also the thick walled cylinder equation to calculate circumferential stress. However, [49] stated Inconel as the sleeve material, which has a Poisson's ratio of circa 0.3. Without adjusting the equation from [16], errors will be induced using Inconel. Reference [49] also stated that due to non-uniform stress distribution through the sleeve thickness, a de-rating factor was used to accommodate peak stress locations within the sleeve. This limited the maximum circumferential stress to reduce the risk of failure. Reference [54] referenced centripetal force equations from [16], which are acceptable if the magnet is constructed using individual blocks and if the sleeve is relatively thin. Reference [54] used segmented magnets, but not many small segments and only one of the two FEA models had a thin sleeve. Lastly, [53] took circumferential

stress and contact pressure equations (due to shrink fitting) from [16] but overlooked referencing. Therefore, [53] used thin cylinder equations and assumed rigid magnets which is a significant simplification of rotor stress behaviour. [5], [46], [55], [56] all used the thin cylinder approximation within their calculations.

Reference [38] dismissed standard equations and justified this with four points:
Their model includes a sleeve laminated axially, using glue to bind the layers.

1. Their magnet material is different to the shaft and sleeve.
2. Their magnets are axially segmented.
3. Their magnets are segmented circumferentially.

For point 1, a thin disk approximation could be used on each sleeve layer, with a correction for the interaction between the layers. For points 2 and 3, standard equations can account for different materials and magnets segmented axially can be analysed using standard equations. Regarding point 4, the standard stress calculations are valid for circumferentially segmented magnets provided that they do not go into circumferential tension. This is the case for [38] as they require a high compressive stress to withstand operating centrifugal forces on the rotor. Reference [47] used a rotor with a solid shaft as the inner radius value is zero. Implementing this, their interference pressure equation and the radial and circumferential stress equations for the assembly at standstill match the equations used by many others (see for example [8]), but the interference pressure equation is missing the magnet Young's modulus. An equation to calculate the total radial stress (a compressive stress) in the magnets is then created. However, focussing on circumferential stress would be more relevant due to the magnets being weak in tension. Reference [45] used a similar approach to [16], but made improvements. The constant Poisson's ratio was removed, but the equation remained unsuitable for orthotropic composite materials.

II. Finite Element Analysis Techniques

Finite element analysis (FEA) is a well-established, computer-based stress analysis method. Models are analysed using an assembly of a finite number of elements to approximate the load-displacement (and hence stress) relationship within complex geometries. Boundary conditions applied to the model will typically include constraints as well as loads. Results accuracy cannot be guaranteed as operating conditions may be difficult or impossible to accurately replicate. For a given geometry and boundary conditions, the FEA stress approximation can be improved by increasing the number of elements. However, this increases the computational time significantly, making FEA potentially very time consuming.

FEA models of rotors can be categorised according to the number of dimensions considered and the extent of the geometry included, as follows:

- 2-Dimensional
  - Full axial cross section
  - Symmetrical axial cross section
- Axisymmetric
  - Full longitudinal section
  - Part longitudinal section
- 3-Dimensional
  - Full geometry
  - Symmetrical section

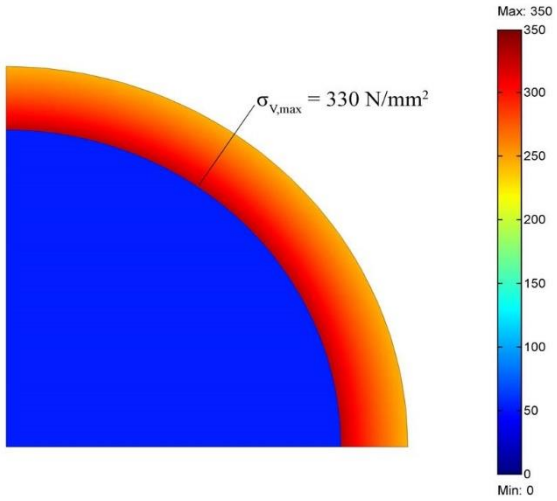

Fig. 4. 2-D Section [52]

2-dimensional models use a cross section of the rotor perpendicular to the rotor axis, as shown in *Fig. 4*. Full face or symmetric sections can be used for the analysis using appropriate boundary conditions. 2-D models process much quicker than 3-D as simpler and fewer elements are used. However, disadvantages of 2-D methods are the stress behaviour must be: assumed to be the same along rotor length; and assumed as either plane stress or generalised plane strain. This creates a source of results unreliability as it was established in [8] that stress changes along the axial direction.

References [3], [15], [21], [23]-[25], [35], [48], [52]-[54] used 2-D FEA, but do not discuss the reasons for this. They also did not specify if their analyses have been made with the same assumptions used in their theoretical calculations i.e. plane stress; plane strain. This makes it difficult to understand if the FEA results are representative of the theoretical conditions. It is clear that [3], [21], [24], [48], [52]-[54] used a 2-D section as their FEA model whereas [15], [23], [25], [35] stated 2-D FEA was used without giving details of the models used. This can make it difficult to replicate and validate the result produced. Reference [15], [21], [23]-[25], [35], [48], [52], [54] achieved good alignment with their analytical calculations however, good agreement between analytical and FEA results does not guarantee accurate results. For example, if both the theory and the FEA make the plane stress assumption then results will agree, but will contain inaccuracies due to the plane stress theory.

There was difficulty in confirming the FEA details reported by [16], [36], [43]-[45], [48], [49], [53], [54], [56]-[59]. There was no mention or justification of the FEA being 2-D or 3-D, or if a plane stress or plane strain assumption was used. References [16], [36], [43]-[45], [48], [54] obtained good agreement with analytical results but as discussed earlier, this does not necessarily equate to result accuracy. References [56]-[59] relied on FEA alone to collect stress results, without verification. Reference [44]

stated that their FEA verified the analytical equations, with an error of 0.21% for the stresses due to interference and temperature. It appears that [45] conducted separate analyses for the magnets and sleeve, while using a hand calculated contact pressure value as a boundary condition. Other boundary conditions or mesh size were not stated, with the FEA appearing to be processed without boundary constraints. Reference [48] doesn't indicate the conditions used in the 2-D FEA setup, but they compared the results with the analytical results; obtained via the use of equations in [16]. This comparison showed a potential error of circa 5%. However, [16] contained both thick shell and thin shell equations, but [48] did not specify which equations were used. Therefore, it is unclear what assumptions were used to generate the results. No boundary conditions, mesh densities or convergence studies are provided by [49], [53], [54]. Also, [49] showed a substantial difference between the analytical and FEA results. Reference [54] highlighted that the thinnest sleeve results agreed most with analytical results due to using the thin cylinder assumption. Using the thick cylinder approach would be required to gain accuracy with thicker sleeves. Both [56] and [57] omit statements regarding dimensionality or boundary conditions. The lack of FEA details in many papers makes it difficult for results to be replicated.

A 2-D axisymmetric model, as shown in *Fig.5*, uses a cross section of the rotor length wall thickness. When revolved around the central axis, the full cylindrical model is complete. A benefit of this method is that stress changes along the rotor length are simulated. However, a limitation is the assumption that stress doesn't change in the circumferential direction. As stated by [8], this condition is true for cylindrical or closely packed magnets whilst the sleeve maintains a compressive stress. The condition is not appropriate where there are gaps between the magnets as shown in [16].

Only [8], [39] used an axisymmetric model in their FEA. It appears that [27] may have also used an axisymmetric model but did not explicitly confirm it. Neither [27] nor [39] stated the constraints used on the analysis, but [39] obtained FEA results agreeing with analytical results, most within 5%. At 150°C and 600,000rpm however, the radial stress error was circa 25%. The agreement adds confidence to the results but without the constraints used on the analysis, the results become difficult to replicate and verify.

The 3-D method usually analyses a 3-D rotor section, as shown in *Fig.6*, with symmetry conditions to replicate full rotor behaviour. Symmetry conditions allow rigid body motion to be eliminated without approximating connection to other parts of the electric machine. A 3-D model removes the need for stress distribution assumptions, as required in 2-D models. However, larger numbers of more complex elements are required to obtain results as accurate as those from 2-D analyses. This significantly increases the processing time and should only be used if necessary.

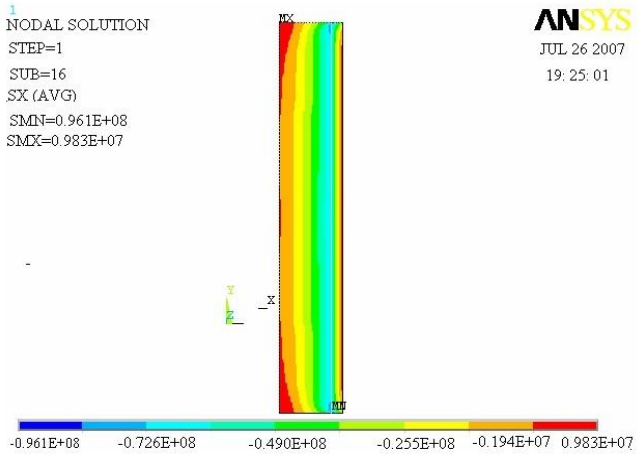

Fig. 5. 2-D Axisymmetric [27]

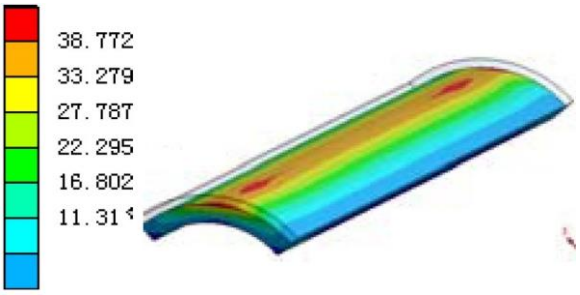

Fig. 6. 3D Sections [60]

References [9], [15], [18], [21], [26], [34], [35], [60], [61] used 3-D FEA models. Reference [35] justified using 3-D over 2-D models due to magnet segments and axial stress distribution not being considered by 2D analysis. However, [8] states 2D axisymmetric FEA is an acceptable model while a compressive circumferential stress is maintained within the rotor. This model would also show the axial stress distribution. Reference [15] used 3-D FEA as a final verification of the 2-D FEA results. Differences in results were found in the magnet inner surface stress due to press-fit; and in the stress at the iron shaft and glass fibre boundary. As noted in [8], stress predictions at these interfaces are very sensitive to mesh density. In [15] the mesh density and boundary constraints were not specified. Reference [18] used a 3-D model to investigate the cause of a magnet failure. The 3-D model showed the high shear stress towards the end of the rotor, causing failure. This high shear stress was also identified by [8] using an axisymmetric model, showing that the 3D model may have been unnecessary. No other variation was seen that required a 3D model over axisymmetric. Reference [60] stated the temperature and rotor speed use in FEA, but did not explain why a 3-D model was used or the constraints applied. Reference [9] also did not explain boundary conditions or provide mesh details. In [9] the plain strain analytical results are compared to 3D FEA results and to a plane stress analytical model. The maximum error between the 3D FEA and the plain strain results was less than 4%. However, when comparing to plane stress results, larger differences were found, in particularly at the shaft. In the shaft, errors of over 1000% were found. Reference [9] attributed this to the plane stress model ignoring axial stress. This could be significant for mechanically weak magnets.

Reference [62] stated that an elastic body subject to loads in three dimensions will result in a 3-D system of stresses, but [8] discussed that 3-D FEA models are not a necessity to be able to explore stresses in three directions. Reference [62] provided no FEA boundary conditions and did not verify the results against an analytical model or practical test. Reference [21] used 3-D FEA to verify analytical and 2-D section FEA results. Of the four locations of stress, the analytical results had an average 21% difference from the 3D FEA and 29% from the 2D FEA model. The plane stress condition was used for the analytical approach after concluding the difference between plane stress and plane strain was negligible, but any constraints on the 2D FEA model were not mentioned. Lastly, [35] used 3-D FEA due to magnet configuration. Segmented magnets with fillers were used which would cause a change in circumferential stress and require the use of 3-D FEA. However, the boundary conditions and mesh details were not discussed. Axial stress was also not incorporated into the analytical calculations.

III. Thermal Analysis

Automotive air-handling machines, such as electrically assisted turbochargers, are exposed to high temperature during operation. The heat is mainly from turbine exhaust gases but also includes heating through compression of the charge air. This also applies to other compressor applications, e.g. vacuum cleaners. Therefore, thermal effects must be accounted for in stress analyses.

References [3], [5], [8], [9], [15], [16], [21], [23], [24], [27], [35]-[37], [39], [44], [45], [48], [49], [52], [56], [58]-[60] all incorporated thermal effects in their analyses, either through analytical calculations or FEA. Of these, [3], [8], [9], [15], [16], [21], [23], [24], [27], [33], [35]-[37], [39], [44], [45], [48], [49] included thermal analysis in the analytical calculations, where [3], [44], [45], [48], [49] and [37] all took the equations from [16] and [27] respectively.

References [3], [8], [9], [15], [16], [21], [23], [24], [27], [33], [35]-[37], [39], [44], [45], [48], [49], [52], [56], [58]-[60] all used uniform rotor temperatures when analysing rotor stresses at elevated temperature, but only [8], [15], [39] justified this decision. [15], [39] both stated that the temperature can be assumed to be constant throughout the rotor, while [8] went further to acknowledge temperature change along the axis. However, this change is small and temperature is constant per axial section. Reference [8] discussed that rotor temperature is constant in the radial and circumferential directions due to poor heat transfer across the air gap between rotor and stator. The largest heat transfer will be along the rotor shaft, causing the axial temperature variation. References [3], [24], [60] also stated that there will be poor heat dissipation from the rotor.

It is important to include thermal effects in the analysis of rotors where their structural integrity relies on interference between parts. Where these parts are made from different materials (e.g. the sleeve and the magnets), it is likely that those materials will have different coefficients of thermal expansion. Hence, even uniform changes in temperature within the rotor will alter the degree of interference between parts. Hence, structural integrity may be compromised due to temperature variations.

IV. Stacked Cylinder Calculations

When calculating stresses in rotors, the boundary layers between cylindrical bodies normally experience the peak stresses. Therefore, it is important to predict these values accurately. All papers bar [40] acknowledge this interaction between the layers. Reference [40] focused on electromagnetic performance.

Of all the papers conducting stress analysis, only [9], [21], [25], [35], [36], [58], [61] incorporated more than two cylindrical bodies in the calculations. Of these, only [9], [25], [35] completed the analysis with closed form calculations, the rest used FEA. Being able to complete these calculations analytically is much more efficient than using FEA, particularly where stresses at the interfering surfaces are being found. References [9], [25], [35] incorporated three cylinders in their models but assumed a state of plane stress. As discussed earlier, the plane stress assumption may produce unreliable results due to ignoring the existence of axial stress.

The review into this aspect of the research highlighted the need for further work in producing analytical equations incorporating three cylindrical bodies that represent rotors in operation. The generalised plane strain condition for three stacked cylinders requires investigation.

V. Optimisation

When conducting rotor stress analysis, the reason is to either assess structural integrity or perform rotor optimisation. Papers [3], [8], [15], [22], [27], [45] focused on or significantly included rotor optimisation with a variety of constraints and criteria being used to define the optimum solution.

To perform optimisation, four categories of parameter are required:

- Criteria
- Design variables
- Constraints
- Fixed design parameters

Criteria must be established as the basis for optimisation and they are the overall goal of the optimisation process. Design variables enable experimentation of different design features to determine an optimal design. Constraints set the limits in which the optimisation process can work and fixed design parameters are user defined specifications that must remain a fixed value. By combining these aspects, users can create an optimal rotor for their specific operating conditions.

Of the papers reviewed, [3], [8], [22], [27], [45] all selected a criterion of minimising the sleeve thickness. Reference [3] also included minimising the magnet thickness as part of the criteria. The benefits of a thinner sleeve are: reduced effective air gap; lower circumferential stress due to rotation; smaller volume; and lower mass. These factors contribute to a more efficient rotor, through both mechanical and electromagnetic performance. Only

[15] opted for an alternative criterion which was to maximise rotational speed. Reference [15] chose their criterion based on a pre-determined electromagnetic design which fixed the effective air gap. Therefore, it appears that rotational speed was focussed on to maximise electromagnetic power output as the sleeve thickness would not affect the effective air gap dimensions.

There was also consensus between papers on the design variables used in the optimisation process. All six papers [3], [8], [15], [22], [27], [45] used interference as a design variable. The level of interference between cylinders has a large impact on rotor stresses and magnet compression. Changing interference enables users to identify a specific value suitable for specific rotor operating conditions. As well as being the criterion for the majority of papers, sleeve thickness was also a common design variable, used by [8], [15], [22], [27], [45]. Sleeve thickness is required to work in conjunction with the interference fit and changes in thickness can alter rotor stresses significantly. Reference [3] did not specify sleeve thickness as a design variable because the outer diameter of the rotor was fixed before optimisation. The magnet thickness was used as the design variable instead, which when changed, determined the sleeve thickness of the rotor. Reference [27] also used magnet thickness as a design variable, which would change the electromagnetic performance of the rotor. Reference [3] also used sleeve material as a design variable and was the only paper to introduce fixed design parameters: rotor outer diameter; and air gap flux density. Fixing design parameters will typically restrict the range of feasible designs and hence could eliminate designs which perform better in terms of the optimisation criteria. Placing minimum and/or maximum limits on design variables will avoid this restriction.

Constraints applied to the optimisation process can be broken down into three categories:

- Criteria Constraints
- Design Variable Constraints
- Functional Constraints

Criteria and design variable constraints are user defined limits imposed on the range of said aspects. Functional constraints are specified limits based on other calculated parameters which are not criteria. In order to generate a feasible design, the design must fall within all the constraints. The optimal design, or designs, will then fall within this feasible set.

As discussed earlier where [8], [15], [22], [27], [45] specified the sleeve thickness as a design variable, they also placed constraints on this dimension. For example, [8] constrained the sleeve outer radius to a range of 13 - 14.5mm, whereas [15] imposed a specified maximum sleeve thickness of 2mm. Reference [3] fixed the rotor outer diameter, but did not constrain the magnet thickness, while [22] did not specify any limitations to the sleeve thickness. This also applies to the interference fit where [8], [27], [45] all defined constraints including interference limits. Reference [15] discussed an optimal interference value being deduced by other constraints and therefore did not include specific constraints on the interference level. Finally, [27] placed limits on the magnet thickness design variable.

All papers [3], [8], [15], [22], [27], [45] stated the sleeve stress must be less than the failure or yield stress. However, it is worth noting that this condition should be applied when the rotor is stationary and in operation. As discussed by [8], the highest compression on the magnets can occur whilst stationary. At speed, the centrifugal forces can expand the sleeve, lowering the compression on the magnets. There are four conditions, stated by [8], where the constraint should be satisfied: minimum speed and minimum temperature; minimum speed and maximum temperature; maximum speed and minimum temperature; and maximum speed and maximum temperature. This ensures the constraint is applied at all times. The sleeve is responsible for keeping the magnets in compression and therefore any failure to the sleeve will result in rotor failure. However, the sleeve stress functional constraint does not ensure the magnets will be held in compression. Therefore, [3], [8], [22] applied a constraint stating there must be a compressive contact pressure between the sleeve and the magnets and [45] specified a range for the contact pressure value. Reference [15], along with [8], stated the inner surface of the magnet must also be in compression. Reference [27] did not apply a contact pressure requirement. Due to the constraints requiring magnets to be in compression, [8], [15], [27] ensured the stress in the magnets could not exceed the maximum allowable stress during operation. This ensures the magnets do not fail due to excessive compression.

Optimisation aims to identify the optimal feasible design. However, without the correct constraints, infeasible designs can be produced. Reference [22] increased the sleeve thickness of their rotor with every optimisation step until the conditions were satisfied. However, with no constraints on the sleeve thickness, if there was a limit to the rotor outer diameter then an infeasible design could have been produced. Both papers [3], [8] identified infeasible designs through their optimisation process, ensuring the final designs were feasible.

References [15], [22], [27], [45] all produced a single feasible optimised design from the optimisation process. Reference [3] identified a set of feasible designs which had a single optimal design for each suitable sleeve material. However, [8] identified a feasible set of designs which satisfied all the constraints. A larger range of designs enables the user to decide which of the feasible designs is most suited to their situation.

There are few papers focusing on optimisation with regard to rotor manufacturing and it would therefore benefit from further research. The majority of papers that included optimisation decided to focus on minimising sleeve thickness as this improves the overall rotor performance. However, without the correct constraints, optimised rotors designs can be produced that cannot be manufactured. For example, excessive interference or very thin sleeve thickness will make rotor assembly difficult. Only [22] mentioned lowering the assembly pressure of the rotor as a target.

VI. Conclusion

Of the 42 papers completing analytical calculations, 23 assumed the plane stress condition. The plane stress

assumption simplifies the equations by ignoring the presence of axial stress but may produce unrealistic results. It is suited to disks or cylindrical objects with a length significantly smaller than the outer diameter. However, rotors for HSEM's typically have longer lengths than outer diameters. The generalised plane strain assumption, which acknowledges the presence of axial stress and strain, provides a more realistic model. As demonstrated by [8], generalized plane strain exists along most of an operating rotor, but plane stress is present at the ends of the rotor. However, this has only been explored by one paper and requires further investigation.

The switch from generalised plane strain to plane stress at the rotor ends has been identified by [18] as inducing a shear effect in the magnets. It has been postulated that this caused a magnet failure but the effect of the shear stress requires further exploration.

The FEA used in the majority of current research used a 2D model. Many papers do not give enough detail about the FEA to confirm what type of 2D analysis it is, or even if 3D FEA has been used. This makes results difficult to validate or replicate externally. Of the 2D analyses, the 2D axial section was the most common method. This type of analysis assumes that there is no change in stress or strain along the axial length of the rotor and would also require plane stress, plane strain or generalized plane strain to be assumed. However, none of the papers reviewed, that stated 2D FEA, specified whether their FEA used the plane stress or plane strain element formulation.

Axisymmetric models appear to be the most suitable method as they don't constrain the stress to be constant along the axis and are still economical. This enables the use of a high mesh density without becoming too large and time consuming to run on the simulation software. However, this type of model would not be suitable where stresses and strains vary in the circumferential direction.

The PM rotors of interest consist of three or four stacked cylinders that contain at least the shaft, magnets and sleeve. The highest stresses occur at the boundary layers, so it is important to accurately predict these stress values. However, only three papers reviewed included analytical calculations for more than two stacked cylindrical bodies and this analysis was restricted to plane stress. Other papers that considered three stacked cylinders used FEA to predict the stresses. Further research is required to evolve calculations to predict stress values based on the generalized plane strain assumption when three or more cylinders are considered.

A small number of papers have aimed to optimise rotor design. Optimization objectives have been: to minimise the sleeve thickness; maximise rotor speed; and minimise total rotor volume. The vast majority of papers sought to minimise sleeve thickness as this would reduce the effective air gap and improve electromagnetic performance. Similar design variables were used and a range of stress parameters were proposed to constrain designs and optimise rotors. While there is some consensus between papers, the lack of sources completing optimisation shows there is more to investigate. Also, very little consideration of manufacturability has been incorporated into the previous optimisation routines from these papers. Robust design optimisation should be the focus of future work.

REFERENCES

[1] A. Tenconi, S. Vaschetto, and A. Vigliani, "Electrical Machines for High-Speed Applications: Design Considerations and Tradeoffs," *IEEE Transactions on Industrial Electronics*, vol. 61, no. 6, pp. 3022-3029, 2014.

[2] M. A. Rahman, A. Chiba, and T. Fukao, "Super High Speed Electrical Machines - Summary," in *IEEE Power Engineering Society General Meeting*, Denver, CO, USA 2004, vol. 2: IEEE, pp. 1272-1275.

[3] H. Fang, R. Qu, J. Li, P. Zhang, and X. Fan, "Rotor Design for High-Speed High-Power Permanent-Magnet Synchronous Machines," *IEEE Transactions on Industry Applications*, vol. 53, no. 4, pp. 3411-3419, July 15 2017.

[4] S. Li and B. Sarlioglu, "Assessment of High-Speed Multi-Megawatt Electric Machines," in *Electric Machines and Drives Conference*, Coeur d'Alene, ID, USA 2015: IEEE.

[5] Z. Kolondzovski, A. Arkkio, J. Larjola, and P. Sallinen, "Power Limits of High-Speed Permanent-Magnet Electrical Machines for Compressor Applications," *IEEE Transactions on Energy Conversion*, vol. 26, no. 1, pp. 73-82, February 18 2011.

[6] C. Gerada, A. Boglietti, and A. Cavagnino, "High-Speed Electrical Machines and Drives," *IEEE Transactions on Industrial Electronics*, vol. 61, no. 6, pp. 2943-2945, June 2014.

[7] D. Gerada, A. Mebarki, N. Brown, C. Gerada, A. Cavagnino, and A. Boglietti, "High-speed electrical machines: Technologies, trends and developments.," *IEEE Transactions on Industrial Electronics*, vol. 61, no. 6, pp. 2946-2959, 2014.

[8] S. Barrans, M. Al-Ani, and J. Carter, "Mechanical design of rotors for permanent magnet high-speed electric motors for turbocharger applications," *IET Electrical Systems in Transportation*, 17th May 2017.

[9] G. Burnand, D. M. Araujo, and Y. Perriard, "Very-High-Speed Permanent Magnet Motors: Mechanical Rotor Stresses Analytical Model," in *Electric Machines and Drives Conference*, Miami, FL, USA 2017: IEEE.

[10] C. Zwyssig, J. W. Kolar, and S. D. Round, "Megaspeed Drive Systems: Pushing Beyond 1 Million r/min," *IEEE/ASME Transactions on Mechatronics*, vol. 14, no. 5, pp. 564-574, September 2 2009.

[11] P. Tsao, M. Senesky, and S. R. Sanders, "An Integrated Flywheel Energy Storage System With Homopolar Inductor Motor/Generator and High-Frequency Drive," *IEEE Transactions on Industry Applications*, vol. 39, no. 6, pp. 1710-1725, 2003.

[12] I. Arsie, A. Cricchio, and C. Pianese, "A Comprehensive Powertrain Model to Evaluate the Benefits of Electric Turbo Compound (ETC) in Reducing CO2 Emissions from Small Diesel Passenger Cars," *SAE Technical Paper Series*, 2014.

[13] N. Terdich and R. Martinez-Botas, "Experimental Efficiency Characterization of an Electrically Assisted Turbocharger," *SAE technical paper series*, 2013.

[14] W. S. Lee, E; Li, Y; Li, S; Bobba, D; Sarlioglu, B, "Overview of Electric Turbocharger and Supercharger for Downsized Internal Combustion Engines," *IEEE Transactions on Transportation Electrification* vol. 3, no. 1, p. 12, 21 October 2016.

[15] A. Borisavljevic, H. Polinder, and J. A. Ferreira, "Enclosure design for a high-speed permanent magnet rotor," in *Power Electronics, Machines and Drives*, Brighton, UK,, 2010: IET.

[16] A. Binder, T. Schneider, and M. Klohr, "Fixation of Buried and Surface-Mounted Magnets in High-Speed Permanent-Magnet Synchronous Machines," *IEEE Transactions on Industry Applications*, vol. 42, no. 4, pp. 1031-1037, October 15 2006.

[17] J. F. Gieras, "Design of Permanent Magnet Brushless Motors for High Speed Applications," in *International Conference on Electrical Machines and Systems*, Hangzhou, China 2014: IEEE.

[18] D. J. B. Smith, B. C. Mecrow, G. J. Atkinson, A. G. Jack, and A. A. A. Mehna, "Shear Stress Concentrations in Permanent Magnet Rotor Sleeves," in *International Conference on Electrical Machines*, Rome, Italy, 2010: IEEE.

[19] R. Keller, E. Mese, and J. Maguire, "Integrated System for Electrical Generation and Boosting (iSGB) " in *International Conference on Electrical Machines and Systems (ICEMS)*, Hangzhou, China, 2014: IEEE.

[20] E. J. Hearn, *Mechanics of Materials 2* (Mechanics of Materials). Oxford, UK: Butterworth-Heinemann, 1997.

[21] F. Zhang, G. Du, T. Wang, G. Liu, and W. Cao, "Rotor Retaining Sleeve Design for a 1.12-MW High-Speed PM Machine," *IEEE Transactions on Industry Applications*, vol. 51, no. 5, pp. 3675-3685, Sept-Oct 2015.

[22] D. Xu, X. Wang, and G. Li, "Optimization Design of the Sleeve for High Speed Permanent Magnet Machine," in *Industrial Electronics and Applications (ICIEA)*, Hefei, China 2016: IEEE, pp. 2531-2535.
[23] L. Chen and C. Zhu, "Rotor Strength Analysis for High Speed Permanent Magnet Machines," in *International Conference on Electrical Machines and Systems (ICEMS)*, Hangzhou, China, 2014: IEEE.
[24] C. Zhu and L. Chen, "Rotor Strength Analysis for Stator-Permanent Magnet Machines," in *International Conference on Electrical Machines and Systems (ICEMS)*, Sydney, NSW, Australia 2017: IEEE, pp. 1-6.
[25] L. Chen and C. Zhu, "Strength Analysis for Surface-mounted Permanent Magnet Rotor in High-Speed Motor," *TELKOMNIKA Indonesian Journal of Electrical Engineering*, vol. 12, no. 10, pp. 7131-7142, October 2014.
[26] W. Cheng, G. Xu, Y. Sun, H. Geng, and L. Yu, "Optimum Design of Ultra High Speed Hybrid Rotor of PM Machines," in *International Conference on Mechatronics and Automation*, Tianjin, China, 2014: IEEE, pp. 1388-1393.
[27] T. Wang, F. Wang, H. Bai, and J. Xung, "Optimization Design of Rotor Structure for High Speed Permanent Magnet Machines," in *International Conference on Electrical Machines and Systems (ICEMS)*, Seoul, South Korea, 2007: IEEE, pp. 1438-1442.
[28] A. Borisavljevic, H. Polinder, and B. Ferreira, "Overcoming limits of high-speed PM machines," in *International Conference on Electrical Machines (ICEM)*, Vilamoura, Portugal 2008: IEEE, pp. 1-6.
[29] P. Pfister and Y. Perriard, "A 200 000 rpm, 2 kW Slotless Permanent Magnet Motor," in *International Conference on Electrical Machines and Systems*, Wuhan, China 2008: IEEE, pp. 3054-3059.
[30] A. Borisavljevic, H. Polinder, and J. A. Ferreira, "On the Speed Limits of Permanent-Magnet Machines," *IEEE Transactions on Industrial Electronics*, vol. 57, no. 1, pp. 220-227, 2010.
[31] P. Pfister and Y. Perriard, "Very-High-Speed Slotless Permanent-Magnet Motors: Analytical Modeling, Optimization, Design, and Torque Measurement Methods," *IEEE Transactions on Industrial Electronics*, vol. 57, no. 1, pp. 296-303, 2010.
[32] A. Gilson, F. Dubas, D. Depernet, and C. Espanet, "Comparison of High-Speed PM Machine Topologies for Electrically-Assisted Turbocharger Applications," in *Electrical Machines and Systems (ICEMS)*, Chiba, Japan, 2016: IEEE, pp. 1-5.
[33] N. Uzhegov, E. Kurvinen, J. Nerg, J. Pyrhönen, J. T. Sopanen, and S. Shirinskii, "Multidisciplinary Design Process of a 6-Slot 2-Pole High-Speed Permanent-Magnet Synchronous Machine," *IEEE Transactions on Industrial Electronics*, vol. 63, no. 2, pp. 784-795, January 8 2016.
[34] D. Xu, X. Wang, and G. Li, "Design and Test for High Speed Permanent Magnet Wind Generator and Research on Rotor Protection Measures," in *Industrial Electronics and Applications (ICIEA)*, Hefei, China 2016: IEEE, pp. 2026-2031.
[35] Y. Wan, S. Cui, S. Wu, L. Song, I. M. Milyaev, and S. O. Yuryevich, "Shock-Resistance Rotor Design of A High-Speed PMSM for Integrated Pulsed Power System," *IEEE Transactions on Plasma Science*, vol. 45, no. 7, pp. 1399-1405, July 7 2017.
[36] A. Damiano, A. Floris, G. Fois, M. Porru, and A. Serpi, "Modelling and Design of PM Retention Sleeves for High-Speed PM Synchronous Machines," in *Electric Drives Production Conference (EDPC)*, Nuremberg, Germany 2016: IEEE, pp. 118-125.
[37] D. Gerada, A. Mebarki, R. P. Mokhadkar, and C. Gerada, "Design Issues of High-Speed Permanent Magnet Machines for High-Temperature Applications," in *IEEE International Electric Machines and Drives Conference*, Miami, FL, USA 2009: IEEE, pp. 1036-1042.
[38] J. M. Yon, P. H. Mellor, R. Wrobel, J. D. Booker, and S. G. Burrow, "Analysis of Semipermeable Containment Sleeve Technology for High-Speed Permanent Magnet Machines," *IEEE Transactions on Energy Conversion*, vol. 27, no. 3, pp. 646-653, July 27 2012.
[39] Y. Zhou and J. Fang, "Strength Analysis of Enclosure for a High-Speed Permanent Magnet Rotor," *AASRI Procedia*, vol. 3, pp. 652-660, 2012.
[40] L. Papini, C. Gerada, D. Gerada, and A. Mebarki, "High Speed Solid Rotor Induction Machine: Analysis and Performances," in *International Conference on Electrical Machines and Systems (ICEMS)*, Hangzhou, China, 2014: IEEE, pp. 2759-2765.
[41] B. Riemer, M. Leßmann, and K. Hameyer, "Rotor Design of a High-Speed Permanent Magnet Synchronous Machine rating 100,000 rpm at 10kW," in *IEEE Energy Conversion Congress and Exposition*, Atlanta, GA, USA 2010: IEEE, pp. 3978-3985.
[42] H. Czichos, *Grundlagen der Ingenieurwissenschaften* (Hutte). Berlin, Heidelberg: Springer Verlag, 1989.
[43] B. D. Varaticeanu, P. Minciunescu, and D. Fodorean, "Mechanical Design and Analysis of a Permanent Magnet Rotors used in High-Speed Synchronous Motor," *Electrotehnica, Electronica, Automatica*, vol. 62, no. 1, pp. 9-17, January 2014.
[44] Z. Tao, Y. Xiaoting, Z. Huiping, and J. Hongyun, "Strength Design on Permanent Magnet Rotor in High Speed Motor Using Finite Element Method," *TELKOMNIKA Indonesian Journal of Electrical Engineering*, vol. 12, no. 2, pp. 1758-1763, March 2014.
[45] Z. Huang and J. Fang, "Multiphysics Design and Optimization of High-Speed Permanent-Magnet Electrical Machines for Air Blower Applications," *IEEE Transactions on Industrial Electronics*, vol. 63, no. 5, pp. 2766-2774, April 8 2016.
[46] G. Berardi, N. Bianchi, and D. Gasperini, "A High Speed PM Generator for an Organic Rankine Cycle System," in *Electric Machines and Drives Conference (IEMDC)*, Miami, FL, USA 2017: IEEE, pp. 1-8.
[47] J. Ahn, J. Choi, C. H. Park, C. Han, C. Kim, and T. Yoon, "Correlation Between Rotor Vibration and Mechanical Stress in Ultra-High-Speed Permanent Magnet Synchronous Motors," *IEEE Transactions on Magnetics*, vol. 53, no. 11, October 24 2017.
[48] A. S. Thomas, Z. Q. Zhu, and G. W. Jewll, "Comparison of flux switching and surface mounted permanent magnet generators for high-speed applications," in *Power Electronics, Machines and Drives (PEMD)*, 2011: IET, pp. 111-116.
[49] W. U. Fernando and C. Gerada, "High speed permanent magnet machine design with minimized stack-length under electromagnetic and mechanical constraints," *International Journal of Applied Electromagnetics and Mechanics*, vol. 46, no. 1, pp. 95-109, 22 January 2013.
[50] J. Luomi, C. Zwyssig, A. Looser, and J. W. Kolar, "Efficiency Optimization of a 100-W, 500 000-rpm Permanent-Magnet Machine Including Air Friction Losses," in *IEEE Industry Applications Conference*, New Orleans, LA, USA 2007: IEEE, pp. 861-868.
[51] J. Luomi, C. Zwyssig, A. Looser, and J. W. Kolar, "Efficiency Optimization of a 100-W 500 000-r/min Permanent-Magnet Machine Including Air-Friction Losses," *IEEE Transactions on Industry Applications*, vol. 45, no. 4, pp. 1368-1377, 2009.
[52] C. Zwyssig and J. W. Kolar, "Design of a 100 W, 500000 rpm Permanent-Magnet Generator for Mesoscale Gas Turbines," in *Industry Applications Conference*, Kowloon, Hong Kong, China 2005, vol. 1: IEEE, pp. 253-260.
[53] S. Zhu, M. Cheng, and X. Sun, "Mechanical design of outer-rotor structure for dual mechanical port machine," in *Electrical Machines and Systems (ICEMS)*, Beijing, China 2011: IEEE.
[54] E. Schubert and B. Sarlioglu, "Mechanical Design Method for a High-Speed Surface Permanent Magnet Rotor," in *IEEE Energy Conversion Congress and Exposition (ECCE)*, Milwaukee, WI, USA 2016, pp. 1-6.
[55] H. Mitterhofer and W. Amrhein, "Design Aspects and Test Results of a High Speed Bearingless Drive," in *Power Electronics and Drive Systems (PEDS)*, Singapore, 2011: IEEE, pp. 705-710.
[56] R. Benlamine, T. Hamiti, F. Vangraefschèpe, and D. Lhotellier, "Electromagnetic, Mechanical and Thermal Analysis of a High-Speed Surface-Mounted PM Machine for Automotive Application," in *International Conference on Electrical Machines (ICEM)*, Lausanne, Switzerland 2016: IEEE, pp. 1662-1667.
[57] N. Bianchi, S. Bolognani, and F. Luise, "Analysis and Design of a PM Brushless Motor for High-Speed Operations," *IEEE Transactions on Energy Conversion*, vol. 20, no. 3, pp. 629-637, 2005.
[58] H. Lahne, D. Gerling, D. Staton, and Y. C. Chong, "Design of a 50000 rpm High-Speed High-Power Six-Phase PMSM for Use in Aircraft Applications," in *International Conference on Ecological Vehicles and Renewable Energies (EVER)*, Monte Carlo, Monaco 2016: IEEE, pp. 1-11.
[59] J. Dong, Y. Huang, L. Jin, and H. Lin, "Comparative Study of Surface-Mounted and Interior Permanent-Magnet Motors for High-Speed Applications," *IEEE Transactions on Applied Superconductivity*, vol. 26, no. 4, 2016.
[60] T. Wang, G. Du, Z. Yu, F. Zhang, and Z. Bai, "Design and Develop of a MW Direct Drive Highspeed Permanent-Magnet Machine for compression," in *International Conference on Electrical Machines and Systems (ICEMS)*, Busan, South Korea 2013: IEEE, pp. 892-895.
[61] N. Uzhegov, J. Barta, J. Kurfurst, C. Ondrusek, and J. Pyrhonen, "Comparison of High-Speed Electrical Motors for a Turbo Circulator Application," *IEEE Transactions on Industry Applications*, vol. 53, no. 5, pp. 4308-4317, September 18 2017.
[62] M. Beshrati, K. R. Pullen, J. D. Widmer, G. Atkinson, and V. Pickert, "Investigation of the Mechanical Constraints on the Design of a Super-high-speed Switched Reluctance Motor for Automotive Traction," in *IET International Conference on Power Electronics, Machines and Drives (PEMD)*, Manchester, UK, 2014: IET pp. 1-6.